Nuclear Science and Techniques (2023) 34:109
https://doi.org/10.1007/s41365-023-01260-w

Numerical simulation of tritium behavior under a postulated accident condition for CFETR TEP system

Hai-Xia Wang[1] · Xue-Wei Fu[1] · Wei-Ping Liu[1] · Tao-Sheng Li[1] · Jie Yu[1]

Received: 29 December 2022 / Revised: 27 March 2023 / Accepted: 2 April 2023 / Published online: 26 July 2023

Abstract
China Fusion Engineering Test Reactor (CFETR) is China's self-designed and ongoing next-generation fusion reactor project. Tritium confinement systems in CFETR guarantee that the radiation level remains below the safety limit during tritium handling and operation in the fuel cycle system. Our tritium technology team is responsible for studying tritium transport behavior in the CFETR tritium safety confinement systems of the National Key R&D Program of China launched in 2017, and we are conducting CFETR tritium plant safety analysis by using CFD software. In this paper, the tritium migration and removal behavior were studied under a postulated accident condition for the Tokamak Exhaust Processing system of CFETR. The quantitative results of the transport behavior of tritium in the process room and glove box during the whole accident sequence (e.g., tritium release, alarm, isolation, and tritium removal) have been presented. The results support the detailed design and engineering demonstration-related research of CFETR tritium plant.

Keywords China Fusion Engineering Test Reactor (CFETR) · Tokamak Exhaust Processing (TEP) system · Numerical simulation · Tritium transport behavior · Tritium confinement system · Accident condition

1 Introduction

For CFETR, designed for high safety and acceptability, tritium safety is one of the key issues. Tritium should be well controlled to prevent excess release into the atmosphere and worker exposure. According to the tritium safety principle of CFETR, tritium should be handled in multiple confinements monitored by detritiation systems; this concept has been successfully adopted in tritium facilities worldwide [1–5].

Tritium is expensive and scarce, and tritium experiments are costly and difficult. Therefore, numerical simulation has been used to investigate tritium leakage and diffusion patterns; those studies have demonstrated that tritium migration and removal behavior is almost perfectly reproduced [6–9] and simulated by three-dimensional flow analysis code [10–13].

The Government of the People's Republic of China considered the tritium safety of CFETR important and thus launched the National Key R&D Program of China in 2017 to conduct "Research on digital technology of CFETR tritium plant". As a member of this project, our tritium technology team is responsible for the three-dimensional tritium transport behavior study in the CFETR tritium safety confinement system. If the first physical barrier fails, tritium will leak into the second barrier, such as a glove box. Moreover, the postulated event of a pipeline break in the Tokamak Exhaust Processing (TEP) System of CFETR has been reported in our prior tritium migration and removal behavior studies based on finite element software COMSOL in the glove box [14–16].

A room or a building where the staff works is crucial as the final tritium confinement barrier to the environment. However, few research on tritium behavior with more than one barrier failure has been reported. The purpose of our ongoing research is mainly to (1) investigate tritium mixing and migration in the process room and the glove box under the condition of double physical barrier failure and (2)

This work was supported by the National Key R&D Program of China-National Magnetic Confinement Fusion Science Program (No. 2017YFE0300305).

✉ Hai-Xia Wang
haixia.wang@inest.cas.cn

[1] Institute of Nuclear Energy Safety Technology, Hefei Institutes of Physical Science, Chinese Academy of Sciences, Hefei 230031, China

evaluate the cleanup performance of the detritiation system in the process room. In this paper, tritium behavior after release (initial tritium behavior) and the behavior when the tritium is removed by the ventilation system (removal tritium behavior) are discussed. The results support the ongoing detailed design and engineering demonstration research on CFETR tritium plant.

2 Postulated accident for TEP system of CFETR

2.1 Brief introduction to CFETR TEP system

TEP is one of the most important systems in the inner fuel cycle process of CFETR, and its main design goal is to treat the plasma exhaust gas from the vacuum vessel and recover most of the tritium in the gas. Similar to ITER's TEP system [17], the TEP system of CFETR also uses a three-stage process to treat plasma exhaust gas: front-end processing, impurity processing, and final cleanup processing [18]. The equipment of the front-end processing system is placed in a separate glove box served by a Glove box Detritiation System (GDS), and the other two systems share one glove box with another GDS. Before being released into the environment, the remaining waste gas is temporarily stored in the decay tank. Power Distribution Cabinets (PDCs) are specially equipped to supply power. All the aforementioned subsystems and components of the TEP system are placed in a dedicated process room (Fig. 1).

During normal operation, the process room is under negative pressure (− 100 Pa), provided by the HVAC (heating, ventilation, and air conditioning) system. If contamination is detected in the air, control actions are implemented by the Detritiation Systems (DSs). The ventilation of the affected room is isolated by the detritiation system from the HVAC, and the following measures are undertaken depending on the contamination levels: (a) all personnel are evacuated, (b) the source of contamination is identified and isolated, and (c) the detritiation system is initiated and the depression in the affected room or area is maintained through the DS by a pressure controller and a flow damper.

2.2 Description of postulated accident

The postulated initiating incident is the instantaneous failure of the tritium process line in the front-end processing system at the maximum design flow rate. Because the pressure of the process line is higher than that of the glove box, process gas is released into the glove box. The release causes the tritium concentration to increase rapidly in the glove box. If the glove box system also fails, tritium sprays into the process room along the breach, resulting in the tritium concentration in the process room increasing rapidly.

According to the latest CFETR design, the tritium concentration in the process room equal to or higher than 1 DAC (3.5×10^5 Bq/m^3, alarm set point) would trigger the contamination alarm, resulting in operator evacuation procedures being initiated. In the event of the tritium release exceeding the threshold of 1×10^8 Bq/m^3 (isolation set point), the failed tritium process line would be isolated according to the instructions of the control system, and the DS would automatically isolate the affected sector from the HVAC system and activate the detritiation and depression functions. The DS would purge the contaminated process room by air to decontaminate the room atmosphere, and the design flow rate is 9000 m^3/h. All the aforementioned parameters (i.e., alarm set point, isolation set point, and design flow rate) are provided by the designer of CFETR

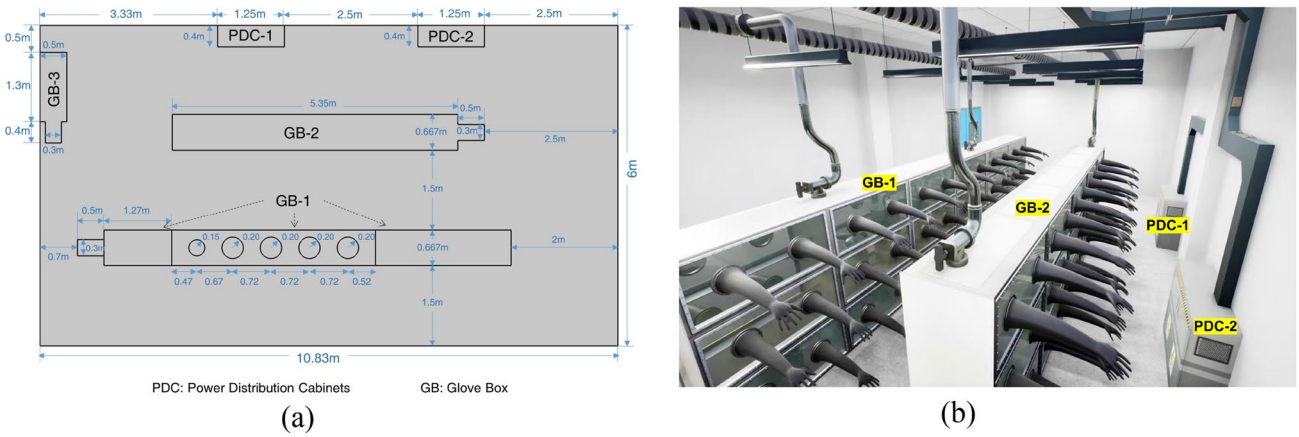

Fig. 1 (Color online) TEP process room. **a** Schematic of TEP process room from top view; **b** 3D virtual geometric scene built by out tritium technology team

tritium plant. The leak route of tritium is as follows: process line >> glove box >> process room >> DS >> environment, and the time sequence of the accident is summarized in Table 1.

Notably, there is a time interval between the moment of the exceeded tritium concentration being detected and the process line isolation and DS initiation. The delay time is designed to be 300 s. Thus, during this 300 s delay, tritium concentration is continuously increasing in the glove box and process room until the DS starts to purge air.

3 Methodology

3.1 Governing equations

The aforementioned accident involves three-level confinement systems: the first barrier is the TEP process line (broken), the second barrier is the related glove box system (failure), and the third barrier is the process room. The leaked tritium transport in the process room, and in the glove box, is essentially the mass transfer issue of the fluid in the flow process. The process complies with the basic equations of fluid control, which are the equations for the conservation of mass, momentum, and energy.

All the released tritium is assumed to be in the form of T_2. Tritium adsorption, desorption, and isotope exchange reactions are not considered in this work. The reason for their exclusion is that the humidity and oxygen content in the glove box and room are designed to be low. The temperature is maintained constant at 295 K during the accident, and no effective heat source is present in the process room. Therefore, considering energy transport is unnecessary. The gaseous fluid velocity in the glove box and process room is smaller than the local sound velocity, and the Mach number (Ma) is well below 0.3 in over 90% of the space. Thus, density changes in that low-velocity gaseous flow can be generally ignored, which means the gaseous fluid is incompressible.

The governing equations for the work gas flow process simulation are expressed as Eqs. 1 and 2. The Navel-Stokes of Reynolds average (RANS) and k-ε turbulence model [19] equations are given as Eqs. 3–6.

$$\nabla \cdot \boldsymbol{u} = 0, \tag{1}$$

$$\frac{\partial \boldsymbol{u}}{\partial t} + \boldsymbol{u} \cdot \nabla \boldsymbol{u} = \boldsymbol{f} - \frac{1}{\rho}\nabla p + \mu \nabla^2 \boldsymbol{u}, \tag{2}$$

$$\rho \frac{\partial k}{\partial t} + \rho \boldsymbol{u} \cdot \nabla k = \nabla \cdot \left(\left(\mu + \frac{\mu_{\mathrm{T}}}{\sigma_k} \right) \nabla k \right) + P_{\mathrm{K}} - \rho \varepsilon, \tag{3}$$

$$\rho \frac{\partial \varepsilon}{\partial t} + \rho \boldsymbol{u} \cdot \nabla \varepsilon = \nabla \cdot \left(\left(\mu + \frac{\mu_{\mathrm{T}}}{\sigma_\varepsilon} \right) \nabla \varepsilon \right) + C_{\varepsilon 1} \frac{\varepsilon}{k} P_{\mathrm{K}} - C_{\varepsilon 2} \rho \frac{\varepsilon^2}{k}, \tag{4}$$

$$P_{\mathrm{K}} = \mu_{\mathrm{T}} \left(\nabla \boldsymbol{u} : \left(\nabla \boldsymbol{u} + (\nabla \boldsymbol{u})^{\mathrm{T}} \right) - \frac{2}{3} (\nabla \cdot \boldsymbol{u})^2 \right) - \frac{2}{3} \rho k \nabla \cdot \boldsymbol{u}, \tag{5}$$

$$\mu_{\mathrm{T}} = \rho C_\mu \frac{k^2}{\varepsilon}, \tag{6}$$

where velocity vector $\boldsymbol{u}$ and pressure p are to be determined in this study. ρ (kg/m^3) represents density and μ (Pa·s) represent dynamic viscosity. $\boldsymbol{f}$ (N) represents force. k (m^2/s^2) and ε (m^2/s^3) represent turbulent kinetic energy and turbulent kinetic dissipation rate, respectively. C_μ, $C_{\varepsilon 1}$, $C_{\varepsilon 2}$, σ_k, and σ_ε are the coefficients of the turbulence model and are listed in Table 2.

During the tritium transport process, there are fluid component transport processes because the leaked tritium is mixed with nitrogen in the glove box and air in the process room. When solving this type of problem, COMSOL predicts the local mass fraction of each component by solving the component transfer equation. The tritium leakage during the whole accident can be predicted to be less than 10% of the glove box volume, and this ratio is even smaller than that

Table 2 Coefficients of turbulent model

Coefficient	Value
C_μ	0.09
$C_{\varepsilon 1}$	1.44
$C_{\varepsilon 2}$	1.92
σ_k	1.0
σ_ε	1.3

Table 1 Time sequence of the accident

Accident sequence	Time (s)
Failure of process line, tritium is released into glove box	0
Tritium sprays into the process room	T_1
Tritium concentration in the process room reaches alarm set point 1 DAC (3.5×10^5 Bq/m^3)	T_2
Tritium concentration in the process room reaches isolation set point 1×10^8 Bq/m^3	T_3
Failed process line is isolated and DS of the process room is activated	T_3+300 s
Tritium concentration in the process room reduced to below 1 DAC (3×10^5 Bq/m^3)	T_4

of the process room. Therefore, considering tritium a dilute substance relative to the background gas (nitrogen or air) is reasonable. The transport process of tritium is described by the convection equation and diffusion equations, Eqs. 7 and 8, respectively.

$$\frac{\partial c_i}{\partial t} + \nabla \cdot \boldsymbol{J_i} + \boldsymbol{u} \cdot \nabla c_i = R_i, \tag{7}$$

$$\boldsymbol{J_i} = -D_i \nabla c_i, \tag{8}$$

where c_i (Bq/m^3) represents the concentration, to be determined in this study. $\boldsymbol{J}_i$ (Bq/m^2·s) represents the diffusion flux vector. R_i (Bq/m^3·s) represents the reaction term, and is set to 0. D_i (m^2/s) represents the diffusion coefficient, and the values were obtained from the literature [8], that of tritium against nitrogen is 5.65×10^{-6} m^2/s and that of tritium against air is 7.41×10^{-6} m^2/s.

Notably, in the process room, only the transport behavior of tritium in the air is considered, ignoring nitrogen leaking from the glove box into the process room. We made this assumption because a) our research object is tritium, b) there is a substantial difference in volume between the glove box (2.62 m^3) and the room (242.09 m^3), and c) 80% of the air is nitrogen; thus, even if the nitrogen in the whole glove box enters the air in the process room, there is little influence on tritium transport in the air. In other words, only one gas species is considered in Eqs. 7 and 8, and the subscript *i* only refers to tritium.

3.2 Geometric model

The information from the China Academy of Engineering Physics (responsible for CFETR tritium plant design) on CFETR TEP system indicates that a three-dimensional geometrical model is built using the geometric kernel of COMSOL (Fig. 2). The inside of the TEP process room is a complete rectangular parallelepiped (10.83 m × 6 m × 4 m), filled with air and controlled at a negative pressure of 100 Pa below atmospheric pressure. In the process room, there are three glove boxes serving (1) the front-end processing, (2) the impurity processing and final cleanup processing, and (3) the gamma decay tank. Additionally, two PDCs stand by a wall: PDC-1 and PDC-2.

There are two simulation domains of interest in this study:

(1) Simulation Domain 1 (SD-1) in the simulation is the whole 3.82 m × 0.667 m × 1.2 m rectangular body in GB-1, filled with nitrogen and controlled at negative pressure of 200 Pa below atmospheric pressure. There is one cylindrical buffer tank (Φ 0.3 m × 0.55 m) and four cylindrical permeators (Φ 0.4 m × 0.8 m), all of which are placed on the ground vertically. The tritium in the TEP process line injects into the glove box through the assumed leak hole (Hole-1), and this hole is set at the top of the second permeator with Φ 0.04 m in the accident.

(2) Simulation Domain 2 (SD-2) in the simulation is the process room space. The tritium in the glove box diffuses into the process room through Hole-2, with Φ 0.04 m located at the front view surface of GB-1 in the accident. The coordinates of Hole-2 are set at (4.178, 1.500, 1.500) after analyzing the possible glove

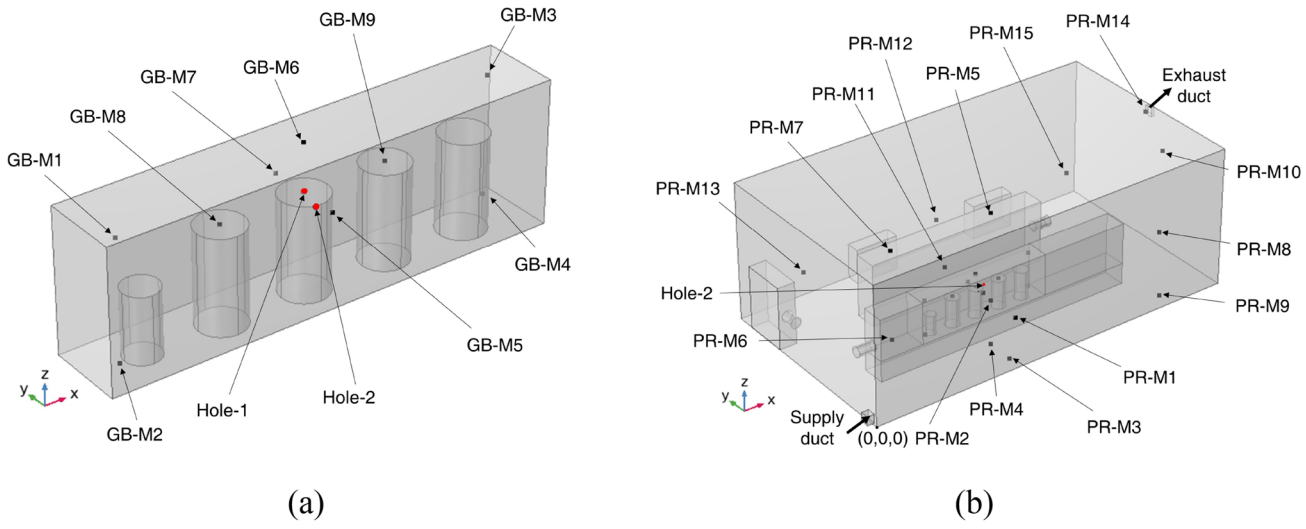

Fig. 2 Three-dimensional geometry model of glove box and process room and locations of monitors and leak holes. **a** Interested part of glove box 1; **b** Process room

damage position due to long-time service. The DS in the process room is assumed to have a supply duct and an exhaust duct in the left and right walls and to operate in the once-through mode with a fixed fluid flow rate.

Nine monitors, from GB-M1 to GB-M9, are set in SD-1 for tritium concentration monitoring. Fifteen monitors, from PR-M1 to PR-M15, are set in SD-2. Table 3 shows the coordinates of tritium leak holes and tritium monitors and the center point of supply and exhaust ducts in the process room.

The basic properties of the working gas nitrogen in the glove box and those of the air in the process room use the parameters provided by the COMSOL material library. The software can automatically set nitrogen density (1.15 kg/m^3) and viscosity coefficient (1.75×10^{-5} Pa·s) according to the working environment of the glove box (295 K, 1 atm—200 Pa = 101,125 Pa). According to the working environment of the process room (295 K, 1 atm—100 pa = 101,225 pa), the air density (1.20 kg/m^3) and viscosity coefficient (1.82×10^{-5} Pa·s) are automatically set as well. The diffusion coefficients of tritium are obtained from the literature [8], and all the parameters have been introduced in Sect. 3.1.

3.3 Boundary conditions and initial values

In the tritium release stage of the accident, the boundary condition at Hole-1 is set as a *velocity* boundary, and the magnitude is given [20] by Eq. 9.

Table 3 Locations of tritium leak holes, tritium monitors, and process room ducts

	x (m)	*y* (m)	*z* (m)	Comments
Tritium release point in process line (Hole-1)	4.330	1.834	1.400	
Tritium release point in glove box (Hole-2)	4.178	1.500	1.500	
GB-M1	2.670	1.700	1.700	
GB-M2	2.670	1.700	0.700	
GB-M3	6.090	1.967	1.700	
GB-M4	6.090	1.967	0.700	
GB-M5	4.330	1.500	1.400	
GB-M6	4.330	1.834	1.800	On the glove-box top wall just above Hole-1
GB-M7	4.330	2.167	1.400	
GB-M8	3.610	1.834	1.400	
GB-M9	5.050	1.834	1.400	
PR-M1	4.178	0.000	1.500	On the process room wall with the same x and z coordinate values as Hole-2
PR-M2	4.178	1.000	1.500	With the same x and z coordinate values as Hole-2, but 0.500 m far away
PR-M3	4.178	0.205	0.205	
PR-M4	4.178	1.000	0.205	
PR-M5	4.178	1.000	4.000	
PR-M6	1.200	1.000	1.500	
PR-M7	1.200	1.000	4.000	
PR-M8	9.630	1.000	1.500	
PR-M9	9.000	0.205	0.205	
PR-M10	9.630	1.000	3.900	
PR-M11	4.178	2.917	1.500	
PR-M12	5.415	4.967	1.500	
PR-M13	1.200	4.850	1.500	
PR-M14	10.730	3.000	3.795	10 cm from the center of the exhaust duct
PR-M15	9.630	4.850	1.500	
Supply duct	0.000	0.205	0.205	
Exhaust duct	10.830	3.000	3.795	

$$v = \sqrt{\frac{2k}{k-1}RT\left[1-\left(\frac{P_2}{P_1}\right)^{\frac{k-1}{k}}\right]} \quad (9)$$

where v represents the leakage velocity, $m{\cdot}s^{-1}$. k represents the gas adiabatic index, which is 1.4. R represents the gas constant, which is 8.314. T represents the temperature, 300 K. P_1 represents the pressure in the tritium process line, 0.25 MPa; P_2 represents the pressure in the glove box, 1 atm–200 Pa. According to the aforementioned values and Eq. 9, the breach velocity is approximately 63.4 $m{\cdot}s^{-1}$.

The walls shared by SD-1 and SD-2 are set as an interial wall and a thin impermeable barrier. The boundary conditions of the other walls are set to wall no slip. Because the DS is not activated in the release stage, the supply vent boundary is set to the wall boundary, and the exhaust vent boundary condition is the pressure boundary with a relative pressure of − 100 Pa. The initial tritium concentrations in SD-1 and SD-2 are both set to 0 Bq/m^3 (Table 4).

In the tritium removal stage, because the tritium stops leaking from the holes, the boundary condition at this point is reset to the wall boundary. The boundary condition at the supply vent is reset to the flow rate boundary, and according to the design of the DS, the flow rate is given as 9000 $m^3{\cdot}s^{-1}$. The walls shared by SD-1 (glove box) and SD-2 (process room), including the one with Hole-2 on it, remain as an interial wall and thin impermeable barrier. The exhaust vent maintains the pressure boundary at a relative pressure of − 100 Pa.

4 Results and discussion

Numerical simulations were performed to investigate the tritium transport performance under fixed ambient conditions and leak apertures (and positions). This paper focuses on the changes in tritium concentration and tritium removal characteristics in the process room (SD-2), which are directly related to the safety of the personnel on site and the tritium amount released into the environment. Tritium behavior in the interest space of GB-1 was also studied to understand the whole process of tritium transport, particularly the changes in tritium concentration in the room. Unless otherwise specified, “glove box” herein is SD-1, not the whole GB-1 or the other two glove boxes.

Table 4 Tritium (T) release conditions

	Glove box	Process room
Chemical formula of tritium	T_2	T_2
Atmosphere	Nitrogen	Air
Humidity	Undetectable	Undetectable
Temperature	295 K	295 K
Pressure	1 atm–200 Pa	1 atm–100 Pa
Ventilation flow rate	–	9000 m^3/h

4.1 Tritium release stage

4.1.1 Contours of tritium concentration

Using the powerful visualization function of COMSOL, Fig. 3 shows the concentration contour maps to observe the three-dimensional evolution of tritium transport. Approximately 0.01 s after the instantaneous failure of the tritium process line, tritium reaches the top of the glove box; the shape of tritium diffusion during this time is similar to a flower bud. Next, this “flower” blooms, and the outer petal symmetrically covers the whole y direction of the glove-box top at 0.026 s. As the tops of the outer petals increase in size and reach Hole-2 at 0.078 s, the symmetry is broken. The “flower” blooming continues, but the tops of the outer petals are destroyed.

The contours of the tritium concentration in the process room are similar to those in the glove box. As shown in Fig. 4, approximately 2.30 s after the accident, the symmetrical outer petal of the tritium “flower” reaches the nearest vertical wall of the process room, and as the top of the outer petals increases in size along the wall, the outer petal symmetrically arrives at the bottom of the wall at 23.67 s. Next, the “flower” continues to move along the wall and the floor, and as the dispersion proceeds, the vortex phenomenon becomes more pronounced.

As shown in Figs. 3 and 4, tritium migrates more quickly along the wall than in space, making it easier to understand the movement of the top petals.

4.1.2 Slices of tritium concentration

Figures 5 and 6 show the slices of tritium concentration. As shown in the first picture of Fig. 5, at the moment of the breach, tritium is quickly ejected from Hole-1 (in the process line) and released to the top of the glove box within 0.01 s, and from this point of view, it resembles a burning candle. The “smoke” generated from this “burning candle" moves approximately symmetrically to the left and right sides and forms an umbrella-shaped "smoke" distribution under the limiting top wall of the glove box. As the release time increases, the tritium concentration increases, and the maximum velocity remains to be observed at the leak hole or, specifically, on the center line of jet flow. At the end of the tritium release stage (300 s), the tritium concentration of the whole glove box reaches $2.36–3.13\times10^{15}$ Bq/m^3.

As shown in Fig. 6, the tritium in the glove box migrates more quickly along the wall than in space. The tritium escapes from the glove box into the process room mainly

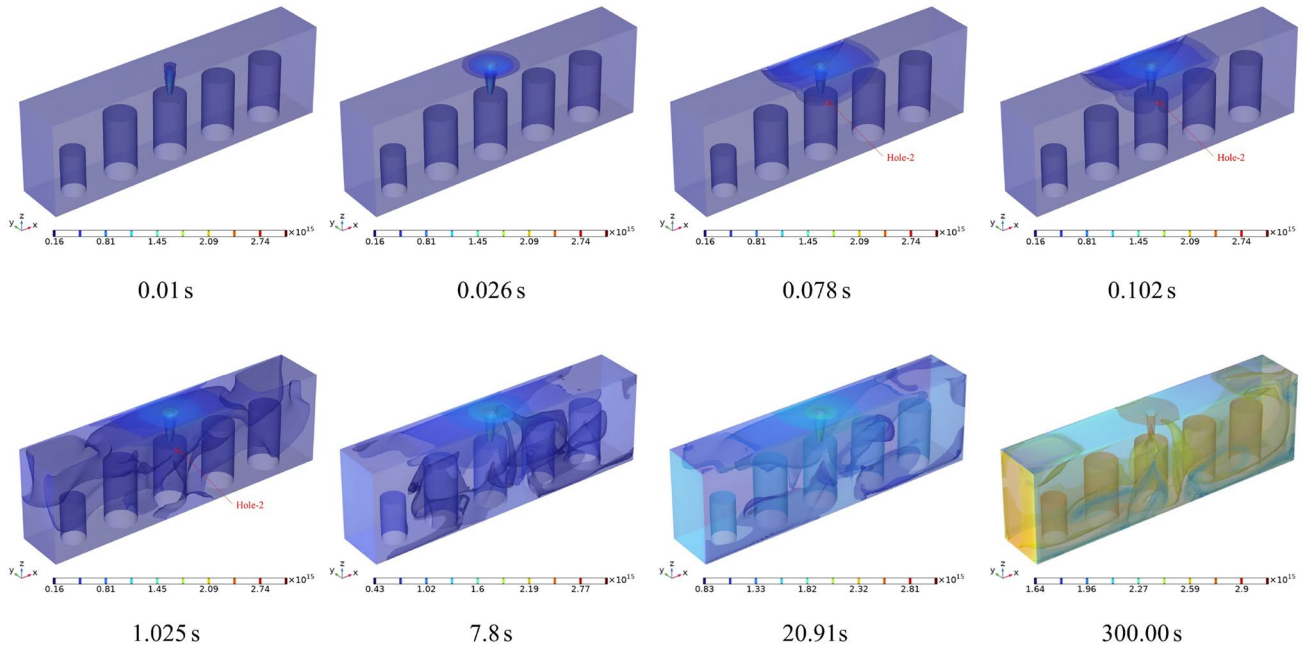

Fig. 3 (Color online) Contours of tritium concentration in the glove box

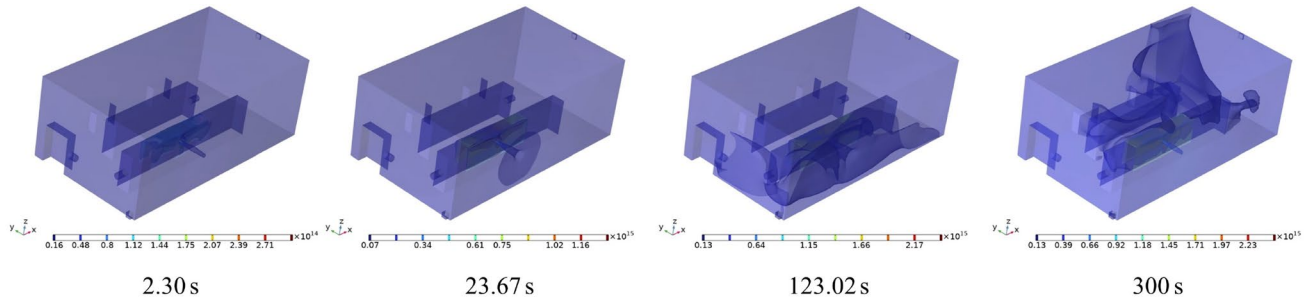

Fig. 4 (Color online) Contours of tritium concentration in the process room

via three routes: (1) tritium is ejected from Hole-1 into the top of the glove box and migrates along the -*y* direction and then down into Hole-2; (2) tritium is injected into the top of the glove box and migrates along the + *y* direction and other directions, and then down into the bottom of the glove box and up into Hole-2; and (3) under the gradient drive of concentration and velocity, tritium in the space of the glove box moves into Hole-2.

4.1.3 Concentration of monitoring points

The variation in tritium concentration at monitoring points might provide more quantitative information from the perspective of safety. Figure 7a shows the variation in tritium concentration from 0 to 300 s at nine monitoring points in the glove box. The conclusions drawn from Fig. 7a are as follows:

1. The trend of tritium concentration is similar at all monitoring points. There is a rapid climb from 0 to $1\times10^{14-15}$ Bq/m^3 during the first 2.5 s, and then tritium concentrations at all monitoring points increase slowly. After approximately 60 s, the tritium concentration basically tends to a constant value. Two groups are formed: $1.63–1.73\times10^{15}$ Bq/m^3 and approximately $2.57–2.63\times10^{15}$ Bq/m^3.
2. At the initial stage, the tritium concentration in GB-M6 is the highest, followed by GB-M5/ GB-M7. At less than 0.06 s, the concentration in GB-M6 and GB-M5/ GB-M7 exceeded 10^{10} Bq/m^3. These phenomena are easily understood because GB-M6 is at the top of Hole-1, and GB-M5/GB-M7 is on the wall very close to Hole-1. For GB-M5 and GB-M7, two spatial symmetry points of the process line breach, the tritium concentration basically shows a uniform step, and the former is closer

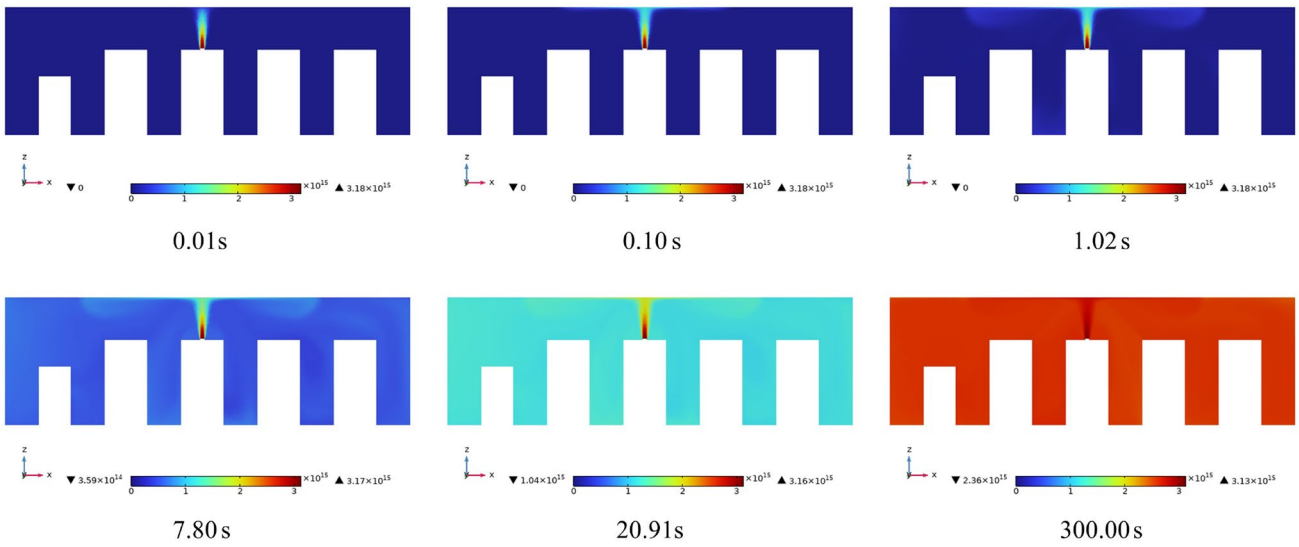

Fig. 5 (Color online) Glove box tritium concentration distribution of ZX slice with $y = 1.800$ m

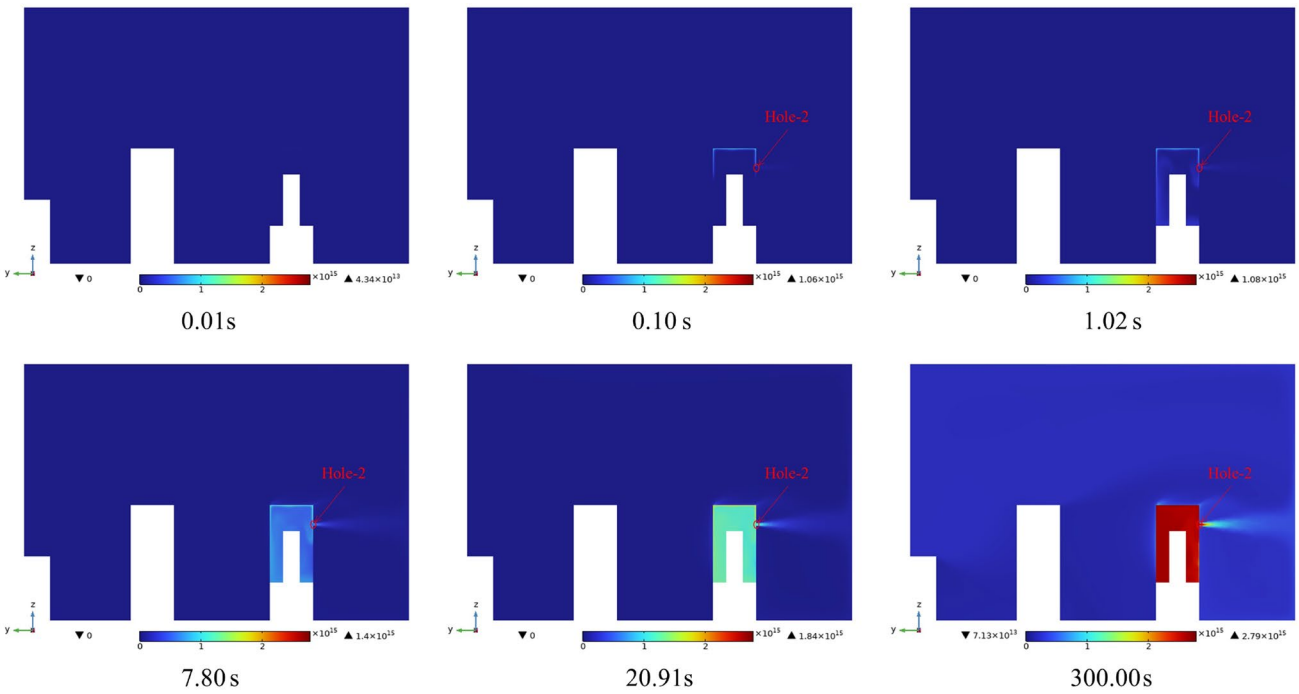

Fig. 6 (Color online) Tritium concentration of YZ slice with $x = 4.178$ m (the same x-coordinate as Hole-2)

to Hole-2 than the latter one, making the concentration at the former a little higher than the latter in a certain period. A similar phenomenon was observed in [10]: the concentration at the monitoring points under the open space condition is slightly larger than that under the closed space condition because the closed boundary suppresses tritium diffusion.

3. GB-M1 and GB-M3, and GB-M2 and GB-M4, are almost two groups of spatial symmetry points and far from Hole-1 and Hole-2. The variation in tritium concentration shows the uniform changing pattern for the symmetrical points of each group. GB-M8 and GB-M9 are perfect symmetry points, and the change

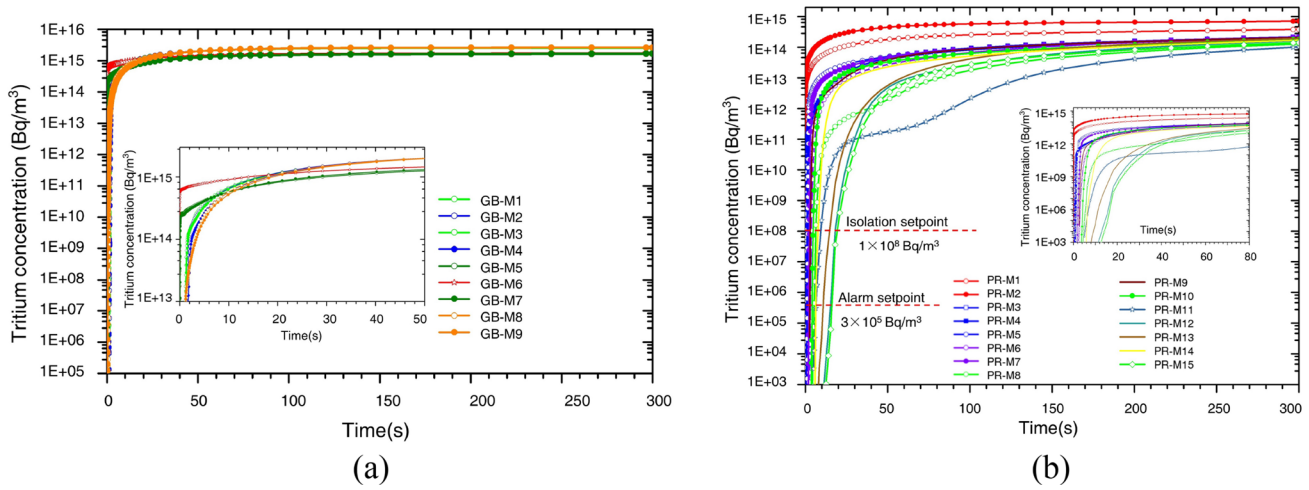

Fig. 7 (Color online) Tritium concentration of monitoring points in tritium release stage. **a** In the glove box; **b** In the process room

lines for the concentration at these points almost coincide.

4. Notably, there is a concentration inversion. In the first 4 s, concentrations at GB-M6 and GB-M5/GB-M7 are higher than those at the other six monitor points. However, after 23 s, the concentrations at GB-M6 and GB-M5/GB-M7 are obviously lower than those at the other monitor points. The possible reason for this finding is that tritium moves more quickly along the wall than in space. In the first 4 s, the amount of tritium that arrives at GB-M6 and GB-M5/GB-M7 is more than the amount of tritium that escapes into the other monitoring points in the process room (see the cases at 0.10 s and 1.02 s in Figs. 5 and 6). As the tritium concentration increases and the space distribution becomes uniform for the nine monitoring points (see the cases at 7.80 s and 20.91 s in Figs. 5 and 6), more tritium escapes into the process room along the wall after 23 s compared with the other monitoring points.

Figure 7b shows the variation in tritium concentration from 0 to 300 s at 15 monitoring points in the process room. The conclusions drawn from Fig. 7b are as follows:

(1) The trend of tritium concentration is similar at all monitoring points in the process room. The concentration climbs quickly, grows slowly, and then tends to a constant value. Different monitoring points have different change times. The space in the process room is much larger than that in the glove box, and monitoring points are set to be distributed in each representative area. Hence, concentrations at different monitoring points show a relatively dispersed distribution compared with those in the glove box. There is a special monitoring point called PR-M11 between the two glove boxes, and the complex flow field leads to a reduced concentration increase, and this point seems "safer" with the lower tritium concentration because its location between the two glove boxes prevented some tritium from flowing through.

(2) The tritium concentration at PR-M2 is the highest, followed by PR-M1, through the whole tritium release period because it is in the direct route of the tritium that escaped from Hole-2. At the initial stage, the next highest points are PR-M3, PR-M4, and PR-M5, whose concentrations exceed the alarm setpoint (3×10^5 Bq/m^3) within 1.31 s. Due to tritium moving more quickly along the wall than in the space, once the tritium arrives at PR-M5 (on the top wall), which is farther from Hole-2 than PR-M3 and PR-M4, the concentration in PR-M5 increases faster than that of PR-M3 and PR-M4. PR-M7 (on the wall) and PR-M6, and PR-M10 (on the wall) and PR-M8, are two groups showing similar trends as PR-M5 and PR-M3/PR-M4. PR-M12, PR-M13, and PR-M15 are far along the route of tritium migration, and the concentrations at these monitors increase later.

(3) From a safety perspective, the monitoring point with the fastest growth rate of tritium concentration should be selected as a reference, i.e., PR-M2. T_1, T_2, and T_3 in Table 1 are within 0.05 s after the accident. Notably, the tritium continues getting released because of the 300 s time interval between the moment of the exceeded tritium detection and process line isolation, as well as DS activation. Therefore, the tritium concentration continues increasing in the glove box and the process room. At the end of the tritium release stage (300 s), the tritium concentration in the process room reaches $1.02\sim7.05\times10^{14}$ Bq/m^3. Next, the DS in the process

room starts to bring in the air. Notably, the highest concentration range in the process room is approximately 7 times larger than the lowest, and the concentration distribution in the process room is more dispersed than that in the glove box ($1.63 \sim 2.63 \times 10^{15}$ Bq/m^3). This result is observed because the space of the process room is much bigger than that of glove box, monitoring points are scattered among the space, and there are complex obstacles in tritium transport.

4.2 Tritium removal stage

In the tritium removal stage, when the DS is initiated, clean air is gradually blew into the process room and destroys the original tritium distribution pattern in the tritium release stage. The final tritium concentration distribution in the tritium release stage (Sect. 4.1) is the initial tritium distribution in the tritium removal stage. Zero seconds in Sect. 4.2 is the start time of the tritium removal stage, the same as the end of the tritium release stage.

4.2.1 Slices of tritium concentration

As the clean air enters the process room, the tritium concentration in the area facing or near the supply vent decreases first. As shown in Fig. 8, there is a low concentration region at the bottom right corner at 0.2 s; thus, clean air arrives at $x = 4.178$ m (Hole-1) from $x = 0$ m (Supply duct) in 0.2 s, and this region remains as the lowest tritium concentration. Tritium concentration continues to decrease as the amount of penetrated air increases. After 30 s, the concentration distributions are similar or the same (particularly after 500 s) except for the range of the legends. In other words, a relatively stable tritium concentration distribution has been formed, and a new tritium concentration distribution pattern has been established.

4.2.2 Concentration of monitoring points

Figure 9 shows the tritium concentration at monitoring points in the tritium removal stage. Driven by the gradient between SD-1 and SD-2, tritium escaped from the glove box through Hole-2, resulting in a decrease in tritium concentration in the glove box. There is a short period (approximately 20 s) of irregular decline, and then the tritium concentrations at all monitoring points in the glove box become nearly a set of log-linear graphs. There are two groups with similar slopes but different tritium concentrations on the line: one for GB-M6 and GB-M5/GB-M7 and the other for the other monitoring points, the same as the grouping in the tritium release stage.

Tritium in the process room is driven out of the room directly by the purge air, while tritium continues to escape from the glove box into the process room through Hole-2. Notably, the former is dominant, and in Fig. 9b, the tritium concentration shows a decreasing trend. Similar to the glove box, there is a short period (approximately 30 s) of irregular decline in the process room, and then the tritium concentrations at all monitoring points become a set of nearly log-linear graphs. The slope of the line is related to the tritium removal rate, and the greater the slope, the faster the tritium is removed. PR-M2 has obvious advantages in

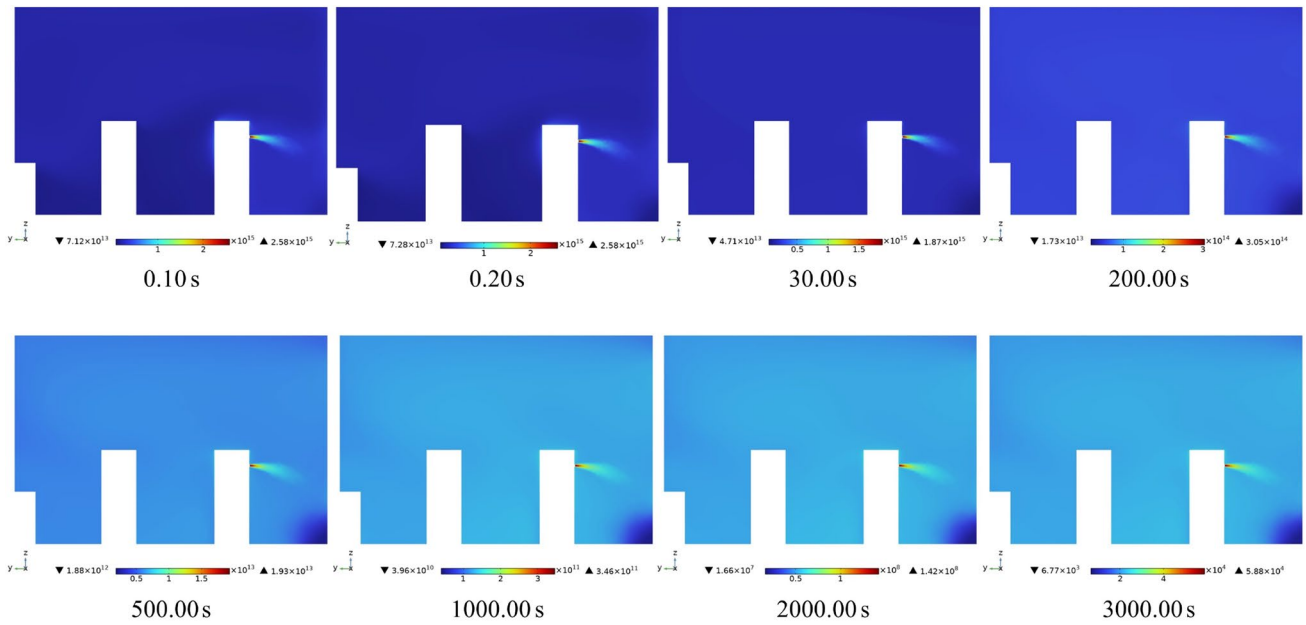

Fig. 8 (Color online) Tritium concentration of YZ slice with $x = 4.178$ m (in the tritium removal stage)

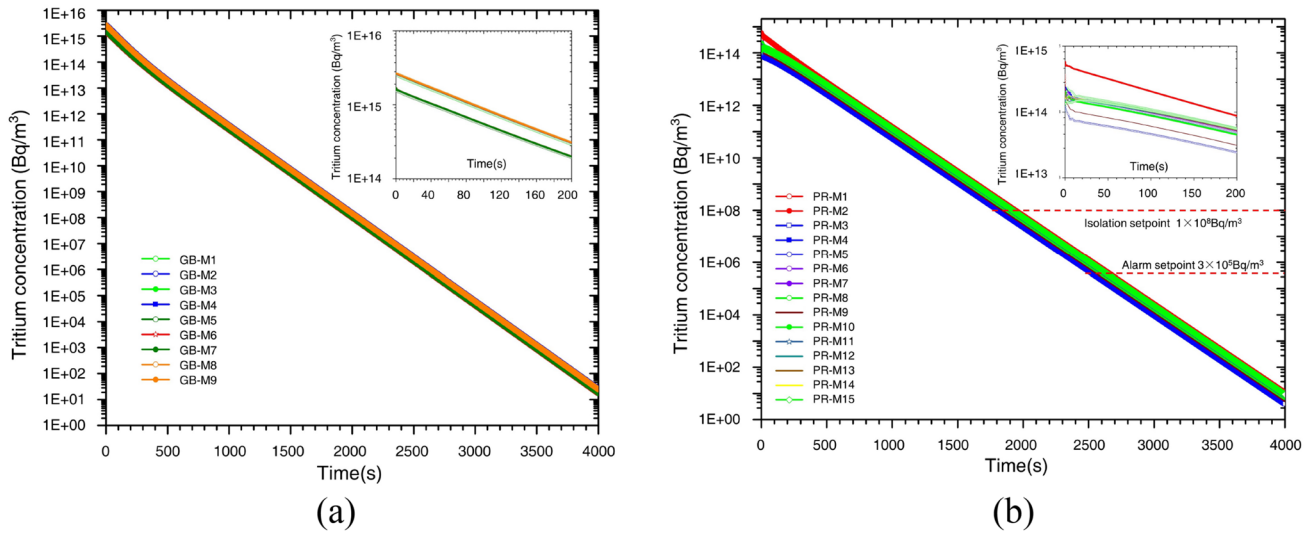

Fig. 9 (Color online) Tritium concentration of monitoring points in tritium removal stage. **a** In the glove box; **b** in the process room

tritium removal rate because the primary flow direction in this location is along the x+ direction, moving to other spaces or the exhaust vent without back-mixing (Fig. 10). PR-M15 has the lowest tritium removal rate, and this result is easy to understand with the streamline in the process room shown in Fig. 10. In this location, the primary flow is characterized spatially as a "spiral flow". PR-M15 seems to be at the center of the spiral, and most of the tritium cannot move to the exhaust vent directly.

The time required for the tritium concentration to fall to the isolation threshold is 1941s, and the time needed for it to fall to the alarm set point is approximately 2667 s (equivalent to T4 in Table 1). The DS continues purge the process room for a longer period of time. When the DS continues working for 3000 s, the maximum concentration among the monitoring points in the process room decreases to 2.61×10^4 Bq/m^3. At 3600 s, the maximum concentration decreases to 243.5 Bq/m^3, less than 1/1000 of the alarm setpoint and 1/100 of the detection limit for general tritium air monitors. Notably, once the DS in the room stops working, the tritium in the glove box will continue to leak, increasing the tritium concentration in the room. However, 1 h of continuous purging decreases the tritium in the glove box and process room to 1.44×10^3 Bq and 4.70×10^4 Bq, respectively (Fig. 11). The ratio of glove box space size to the process room is ~ 1/100 (2.6192 m^3/242.09 m^3); thus, even if all the residual tritium in the glove box entered the room, the effect on tritium concentration in the room would be slight.

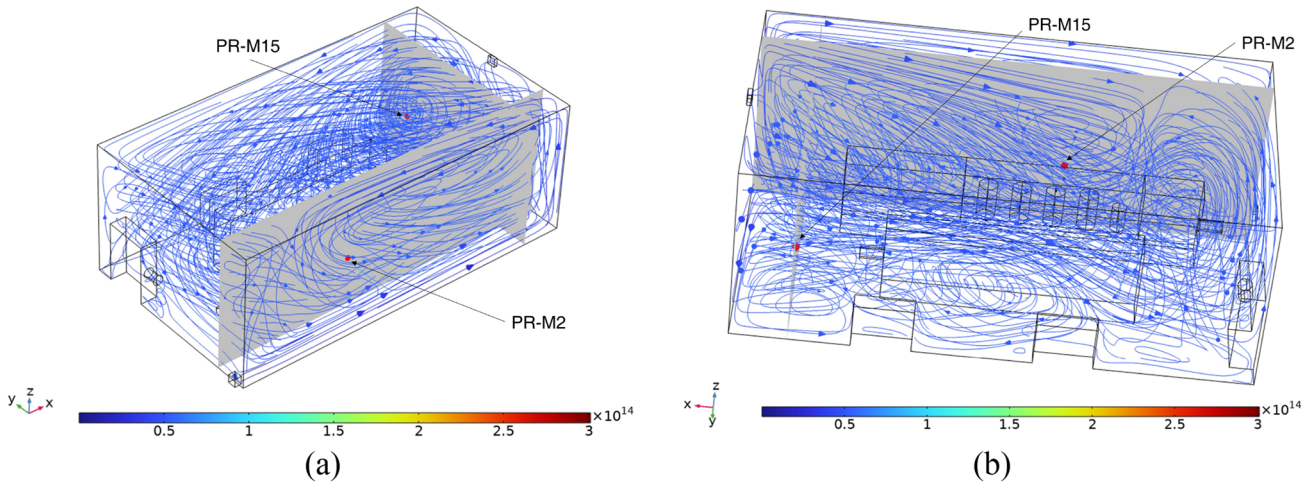

Fig. 10 (Color online) Tritium concentration streamline in process room in tritium removal stage. **a** Visual angle 1; **b** Visual angle 2

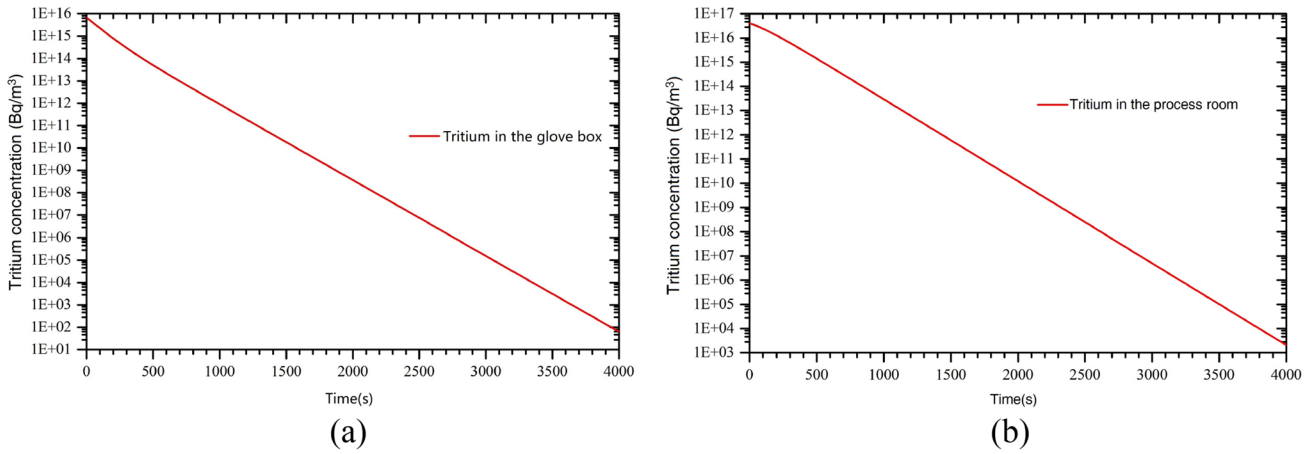

Fig. 11 Total tritium in tritium removal stage. **a** Tritium in SD-1; **b** Tritium in SD-2

5 Summary

A numerical model for the subsonic jet flow of tritium leakage from the process line and the glove box was developed using the software COMSOL to investigate tritium transport behavior under a postulated accident condition of the TEP system for CFETR. This paper was concerned with tritium concentration and tritium removal characteristics in the process room because they are directly related to staff safety on site. Changes in tritium concentration in the glove box were also studied because understanding the whole process of tritium, particularly the tritium concentration changes in the room, is useful.

(1) In the tritium release stage

The tritium concentrations at monitoring points in the process room climb quickly, grow slowly, and then tend to a constant value. This phenomenon regarding the tritium concentration in the glove box is easy to understand because all of the tritium in the room is from the glove box.

The concentration at PR-M2 increases the fastest and remains the highest through the whole time period because it is the closest monitoring point to Hole-2. In an extremely short time (0.05 s) after the accident, tritium concentration exceeded the alarm set point and isolation set point. PR-M2 should be selected as a reference monitoring point from a safety perspective. At the end of the tritium release stage (300 s), the tritium concentration in the process room reaches $1.01–7.05 \times 10^{14}$ Bq/m^3. Subsequently, the DS in the process room starts to purge air.

(2) In the tritium removal stage

When the DS starts working, clean air gradually enters the process room and destroys the original tritium distribution pattern in the tritium release stage. Tritium is driven out of the room by the purge air. The air volume exceeds the tritium volume escaping from the glove box into the process room through Hole-2; therefore, the tritium concentration decreases. There is a short period (within 30 s) of irregular decline, and then the tritium concentrations at all monitoring points become a set of nearly log-linear graphs. The highest tritium removal rate is observed at PR-M2 because there is no back-mixing in this location, and the lowest removal rate is observed at PR-M15 because the primary flow is characterized spatially as a "spiral flow" and little tritium moves to the exhaust vent directly. It takes approximately 1941 s for the tritium concentration to decrease to the isolation threshold and approximately 2667 s to reach the alarm setpoint. An one hour purge might reduce the tritium concentration in the process room to less than 1/1000 of the alarm setpoint and 1/100 of the measurement limit for the general tritium air monitor. After the DS stops working, even if all the residual tritium in the glove box enters the room, the tritium concentration in the room would hardly be affected.

Furthermore, the tritium concentration slices and contours might intuitively represent the movement of spilled tritium in the second and third tritium barriers, which would aid in explaining the process and mechanism of this phenomena. The impact of the emergency system in the process room on tritium transport was observed, and a key time was identified to evaluate the conceptual design of the current tritium removal system to fulfill the tritium safety requirements.

Only the first stage results have been summarized. Many factors affect the tritium transport process, for example, the size, location, and shape of the breach; the location and size of the DS vents; the purge gas velocity and direction; and the response time of the tritium emergency system, et al. A more comprehensive and systematical three-dimensional

numerical simulation than that in this study is being conducted for tritium leakage and diffusion; the results will be reported.

Acknowledgements Special thanks to Jin-Guang Cai and Xiang-Lin Wang from the China Academy of Engineering Physics for providing valuable design information on CFETR tritium plant.

Author contributions All authors contributed to the study conception and design. Material preparation, data collection and analysis were performed by Hai-Xia Wang, Xue-Wei Fu, Wei-Ping Liu, Tao-Sheng Li and Jie Yu. The first draft of the manuscript was written by Hai-Xia Wang and all authors commented on previous versions of the manuscript. All authors read and approved the final manuscript.

Data availability The data that support the findings of this study are openly available in Science Data Bank at https://doi.org/10.57760/sciencedb.j00186.00096 and https://cstr.cn/31253.11.sciencedb.j00186.00096.

Declarations

Conflict of interest The authors declare that they have no competing interests.

References

1. M. Glugla, A. Antipenkov, S. Beloglazov et al., The ITER tritium systems. Fusion Eng. Des. **82**, 472–287 (2007). https://doi.org/10.1016/j.fusengdes.2007.02.025
2. Y.N. Hrstensmeyer, B. Butler, C. Day et al., Analysis of the EU-DEMO fuel cycle elements: intrinsic impact of technology choices. Fusion Eng. Des. **136**, 314–318 (2018). https://doi.org/10.1016/j.fusengdes.2018.02.015
3. X.L. Wang, G.M. Ran, H.Y. Wang et al., Current progress of tritium fuel cycle technology for CFETR. J. Fusion Energ. **38**, 125–137 (2019). https://doi.org/10.1007/s10894-018-0158-1
4. X.C. Nie, J. Li, S.L. Liu et al., Global variance reduction method for global Monte Carlo particle transport simulations of CFETR. Nucl. Sci. Tech. **28**, 115 (2017). https://doi.org/10.1007/s41365-017-0270-3
5. Y. Du, Y. Yang, S.B. Jiang et al., An autocontrol detritiation system. Nucl. Tech. **33**, 233–236 (2010). (**in Chinese**)
6. T. Hayashi, K. Kobayashi, Y. Iwai, et al., Tritium behavior intentionally released in the radiological controlled room under the US-Japan collaboration at TSTA/LANL. Fusion Technol. **34**, 521–525 (1998). https://doi.org/10.13182/FST98-A11963665
7. T. Hayashi, K. Kobayashi, Y. Iwai, Tritium behavior in the Caisson, a simulated fusion reactor room. Fusion Eng. Des. **51**, 543–548 (2000). https://doi.org/10.1016/S0920-3796(00)00214-3
8. Y. Iwai, T. Hayashi, T. Yamanishi et al., Simulation of tritium behavior after intended tritium release in ventilated room. J. Nucl. Sci. Technol. **38**, 63–75 (2001). https://doi.org/10.1080/18811248.2001.9715008
9. Y. Iwai, T. Hayashi, K. Kobayashi et al., Simulation study of intentional tritium release experiments in the caisson assembly for tritium safety at the TPL/JAERI. Fusion Eng. Des. **54**, 523–535 (2001). https://doi.org/10.1016/S0920-3796(00)00581-0
10. W. Li, H.Q. Kou, X.G. Zeng et al., Numerical simulations on the leakage and diffusion of tritium. Fusion Eng. Des. **159**, 111749 (2020). https://doi.org/10.1016/j.fusengdes.2020.111749
11. H.M. Sahin, G. Tunc, A. Karakoc et al., Neutronic study on the effect of first wall material thickness on tritium production and material damage in a fusion reactor. Nucl. Sci. Tech. **33**, 43 (2022). https://doi.org/10.1007/s41365-022-01029-7
12. C.J. Li, X.F. Cai, M.Q. Xiao et al., Analysis on the influencing factors of radioactive tritium leakage and diffusion from an indoor high-pressure storage vessel. Nucl. Sci. Tech. **33**, 151 (2022). https://doi.org/10.1007/s41365-022-01147-2
13. B. Feng, W.H. Zhuo, Levels and behavior of environmental tritium in East Asia. Nucl. Sci. Tech. **33**, 86 (2022). https://doi.org/10.1007/s41365-022-01073-3
14. J.C. Han, H.X. Wang, T.S. Li et al., Simulation study of tritium transport in CFETR TEP glove box based on COMSOL. Nucl. Saf. **21**(5), 72–80 (2022). https://doi.org/10.16432/j.cnki.1672-5360.2022.05.012. (**in Chinese**)
15. H.X. Wang, X.W. Fu, J.C. Han et al., Numerical simulation of tritium behavior in tritium confinement system for China fusion engineering test reactor. Paper presented at the 9th Computational Fluid Dynamics for Nuclear Reactor Safety, Texas A&M University, 20–22 February 2023
16. D.H. Daher, M. Kotb, A.M. Khalaf et al., Simulation of a molten salt fast reactor using the COMSOL multiphysics software. Nucl. Sci. Tech. **31**, 115 (2020). https://doi.org/10.1007/s41365-020-00833-3
17. ITER Organization, *Preliminary Safety Report (RPrS)*. (DAC files, Saint Paul-lez-Durance, 2011)
18. G.M. Ran, J.G. Cai, H.Y. Wang et al., The CFETR tritium plant: requirements and design progress. Fusion Eng. Des. **159**, 111930 (2020). https://doi.org/10.1016/j.fusengdes.2020.111930
19. M. Saeed, J.Y. Yu, A.A.A. Abdalla et al., An assessment of k-ε turbulence models for gas distribution analysis. Nucl. Sci. Tech. **28**, 146 (2017). https://doi.org/10.1007/s41365-017-0304-x
20. G.Y. Liu, Dissertation, University of South China, 2017 (**in Chinese**)